

1-1-1985

Heterodyne Holography Applications in Studies of Small Components

Ryszard J. Pryputniewicz
Worcester Polytechnic Institute, rjp@wpi.edu

Follow this and additional works at: <http://digitalcommons.wpi.edu/mechanicalengineering-pubs>



Part of the [Mechanical Engineering Commons](#)

Suggested Citation

Pryputniewicz, Ryszard J. (1985). Heterodyne Holography Applications in Studies of Small Components. *Optical Engineering*, 24(5), 849-854.

Retrieved from: <http://digitalcommons.wpi.edu/mechanicalengineering-pubs/41>

This Article is brought to you for free and open access by the Department of Mechanical Engineering at DigitalCommons@WPI. It has been accepted for inclusion in Mechanical Engineering Faculty Publications by an authorized administrator of DigitalCommons@WPI.

Heterodyne holography applications in studies of small components

Ryszard J. Pryputniewicz

Worcester Polytechnic Institute
Department of Mechanical Engineering
Center for Holographic Studies
and Laser Technology
Worcester, Massachusetts 01609

Abstract. Heterodyne hologram interferometry was used to study load-deformation characteristics of computer microcomponents that were surface mounted on a printed circuit board. The board was assembled as a cantilever plate and subjected to cyclic flexure loading according to industry standards. The flexure loading was sinusoidal at 0.1 cps with an amplitude of 1.25 mm (0.050 in.) at the tip of the board. Double-exposure heterodyne holograms were recorded under a number of conditions specified by the magnitude of deflection at the board's tip and the number of accumulated flexure cycles. Data obtained during reconstruction of heterodyne holograms were used to compute displacements and strains along the leads connecting the component to the printed circuit board. The experimental results show that lead displacements were on the order of 1.2 μm , while strains were up to 0.054%. The results obtained in this study will be used as input to finite element models of computer microcomponents.

Subject terms: holographic interferometry; heterodyne hologram interferometry; quantitative interpretation of interferograms; strain; displacement.

Optical Engineering 24(5), 849-854 (September/October 1985).

CONTENTS

1. Introduction
2. Method
 - 2.1. Heterodyne hologram interferometry
 - 2.2. Recording and reconstruction of heterodyne holograms
3. Component board assembly and loading apparatus
4. Experimental procedure
5. Experimental results
 - 5.1. Calibration data
 - 5.2. Load-deformation data
6. Conclusions

1. INTRODUCTION

Ever-increasing demands for optimum design of electronic components, in particular in respect to electronic packaging, require accurate knowledge of the behavior of components under actual operating conditions. This information, however, is difficult to obtain experimentally because of the small size of today's electronic components. Also, the conventional experimental procedures involving strain gauges, photoelasticity, mechanical probing, etc., are generally not applicable to these measurements because they are invasive in nature and, therefore, interfere with the performance of the tested component. An alternative to the conventional experimental methods, however, can be provided using recent developments in laser technology.

Out of a number of the existing laser methods available today, the method of heterodyne hologram interferometry was found to be most applicable to the studies of electronic components, as presented in this paper. This stems from the fact that displacements and/or deformations of today's electronic components are very small and take place over the entire component, which itself is very small (on the order of a few millimeters in physical dimensions). Therefore,

methods used to make measurements on such components must assure accurate and precise results. Otherwise, experimental uncertainties will constitute an appreciable percentage of the measured quantity, and the experimental results might not be useful from the designer's point of view.

The results presented in this paper were obtained using the method of laser heterodyne hologram interferometry to study displacements and strains in the leads connecting the component to the printed circuit board. The board assembly that was tested was provided by industry. The assembly was mounted and loaded according to specifications set by the industry. The following sections will detail the method used, the laboratory apparatus employed in the study, and the results obtained.

2. METHOD

In the studies presented in this paper, the method of double-exposure heterodyne hologram interferometry was used. In particular, the double-exposure holograms were recorded in such a way that the first exposure was made with the board assembly at some initial state of stress; then the state of stress was changed and the second exposure was made. Both exposures were made in the same high resolution photosensitive medium. During reconstruction of the double-exposure heterodyne holograms, optical phase measurements were made along each of the component leads. Using these phase measurements, displacements and strains along each of the leads were computed. The fundamental principles of double-exposure heterodyne hologram interferometry are given in Secs. 2.1 and 2.2.

2.1. Heterodyne hologram interferometry

The characteristic principle of heterodyne hologram interferometry is that each of the two object fields (in the case of a double-exposure hologram) is recorded with a different reference beam; these recordings are made in a high resolution photosensitive medium. The reference beams are set up in such a way that they can be reproduced independently during the hologram reconstruction process, with the introduction of a known frequency shift between them. As a result of

Invited Paper HI-112 received March 1, 1985; revised manuscript received April 22, 1985; accepted for publication May 27, 1985; received by Managing Editor June 25, 1985.

© 1985 Society of Photo-Optical Instrumentation Engineers.

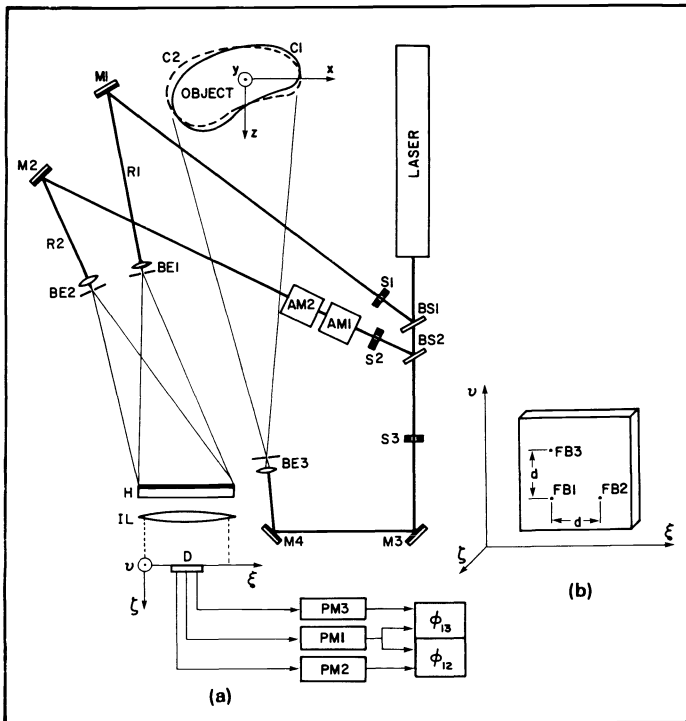


Fig. 1. Heterodyne system. (a) System setup: BS1, BS2—beam splitters; S1 to S3—shutters; AM1, AM2—acousto-optic modulators; M1 to M4—mirrors; BE1 to BE3—beam expanders; R1, R2—reference beams; H—hologram; IL—imaging lens; D—photodetector; PM1 to PM3—photomultipliers; ϕ_{12} , ϕ_{13} —differential phase meters; C1, C2—object configurations. (b) Fiber-optic detector head: FB1 to FB3—fiber-optic bundles; d—center-to-center distance between pairs of fiber-optic bundles.

this, the two reconstructed and interfering light fields are intensity modulated at the frequency equal to the frequency shift between the reference beams. This intensity modulation takes place at all points within the interference pattern produced during reconstruction of the hologram. Now, the optical path differences corresponding to the displacement and/or strain recorded within the hologram being reconstructed are converted into the phase of the beat frequency of the two interfering light fields. This phase is, in turn, interpolated optoelectronically, resulting in highly accurate determination of displacements and/or strains.

2.2. Recording and reconstruction of heterodyne holograms

The setup used in heterodyne hologram interferometry is shown in Fig. 1. In this arrangement, laser output is divided into three beams by means of beam splitters BS1 and BS2. The first beam, reflected from BS1, is directed by mirror M1, via beam expander BE1, toward the recording medium H; this is reference beam R1. The second beam, reflected from BS2, is reference beam R2. The third beam, directed by mirrors M3 and M4, is expanded by BE3 to illuminate the object being studied. This beam, modulated by reflection from the object, is recorded against R1 and R2, one at a time, with the exposure being controlled by shutters S1 and S2, respectively, as described below.

Using the heterodyne holography arrangement shown in Fig. 1, the object's configuration C1, corresponding to its initial state, is recorded using the object beam and R1, while R2 is stopped by S2. Following the first exposure, the state of the object is altered, resulting in configuration C2. Then, the second exposure is made in the same photosensitive medium, recording C2. This second recording, however, is made using the object beam and R2, while R1 is blocked by S1. It should be noted that during the two exposures, the object beam as well as R1 and R2 all have the same frequency.

The exposed photosensitive medium is processed and then reconstructed by simultaneous illumination with R1 and R2, while the object beam is stopped by S3. Now, however, a frequency shift is introduced between R1 and R2 by means of the acousto-optic modulators AM1 and AM2, which are cascaded in R2.

A photodetector D [Fig. 1(a)], placed at a point within the image formed by an imaging lens IL, detects intensity variation in any region where the two light fields overlap. The "observed" intensity is modulated at the beat frequency equal to the frequency difference between the two reconstructing beams.

In the setup used to obtain results presented in this paper, a detector assembly consisting of three fiber-optic bundles FB1, FB2, and FB3, Fig. 1(b), was used. The signals from the fiber-optic bundles were fed into photomultipliers PM1, PM2, and PM3. The outputs from the photomultipliers were, in turn, sensed and displayed by the differential phase meters, as shown in Fig. 1(a). The phase differences were measured at a number of points along each of the leads and were used to compute displacements and strains.

The printed circuit board with surface-mounted components used in this study was assembled and loaded as described in Sec. 3.

3. COMPONENT BOARD ASSEMBLY AND LOADING APPARATUS

The board used in this study was provided by industry. The board was also assembled, loaded, and tested as specified by the industry; it is shown schematically in Fig. 2. The cross-sectional geometry of the printed circuit board, the component, the lead, and the solder, including characteristic dimensions, is shown in Fig. 3.

The board, with mounted components, was assembled as a cantilever plate [Fig. 2(a)] with its upper end free to deflect. The lower end of the board was fixed so that a distance of 6.35 mm (0.250 in.) was maintained between the fixture and the lowermost component [Fig. 2(b)]. Also, a loading device (Fig. 4) was attached in such a way as to provide ± 1.25 mm (± 0.050 in.) deflection (with respect to the board's centerline) at the free end of the board, as measured at a distance of 101.6 mm (4 in.) above the fixture [Fig. 2(b)].

The loading device used in this study consisted of a push rod, a cam, and a motor with a speed control (Fig. 4). The motor's speed was adjusted to obtain a cyclic frequency of 0.1 cps. The cam was designed to provide the cyclic amplitude of ± 1.25 mm (± 0.050 in.). Therefore, the load applied to the component board was sinusoidal with an amplitude of ± 1.25 mm (± 0.050 in.) and a frequency of 0.1 cps. The board assembly, together with the loading apparatus, became a part of the heterodyne holography system.

4. EXPERIMENTAL PROCEDURE

To measure displacements and strains in the leads connecting the component to the board, double-exposure heterodyne holograms were recorded and reconstructed as described in Sec. 2. The first exposure of every hologram was recorded with the board in its unloaded position. Then, the board was deflected a known amount in a known direction [deflection applied to the board was in the direction parallel to the x-axis of the Cartesian coordinate system shown in Fig. 2(a)]. Finally, the second exposure was made with the board in the new position.

Images of the component were magnified $8\times$ during reconstruction of the heterodyne holograms. The phase difference measurements were made by moving the fiber-optic detector head (Fig. 1) in the plane of the magnified image of the component. The detector was moved along the center of each of the six leads by changing its position in increments of 1 mm (as measured in the image space). The direction of scan was from the printed circuit board toward the component, as shown in Fig. 2(c). In this fashion, it was possible to make measurements at 40 points along each lead, including the board-lead solder joint and the lead-component interface.

The data provided by these measurements can be thought of as being equivalent to information that could have been obtained if it were possible to place 40 strain gauges along each lead. In fact, the

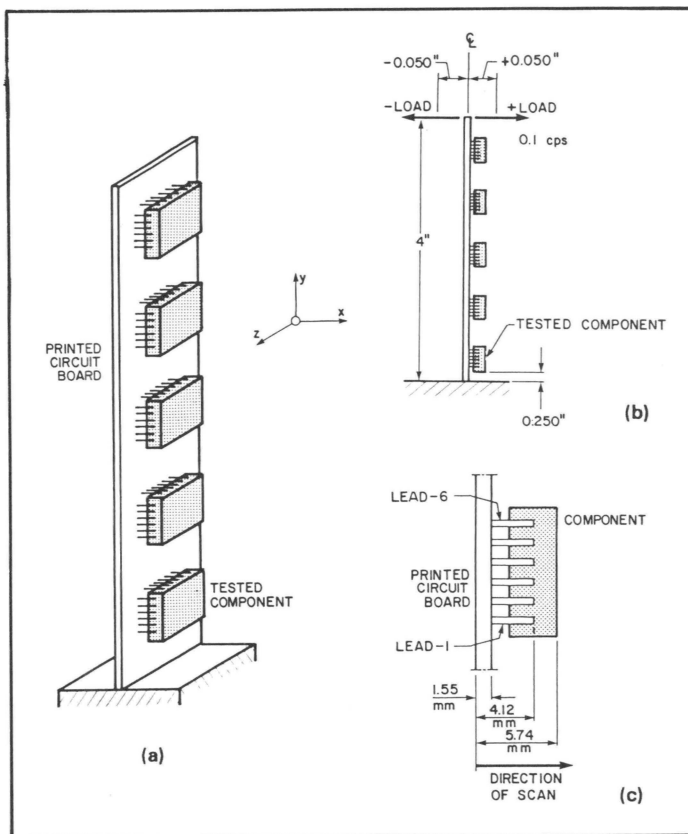


Fig. 2. Printed circuit board and component assembly: (a) component definition and coordinate system, (b) assembly and loading specifications, (c) component geometry and direction of scan.

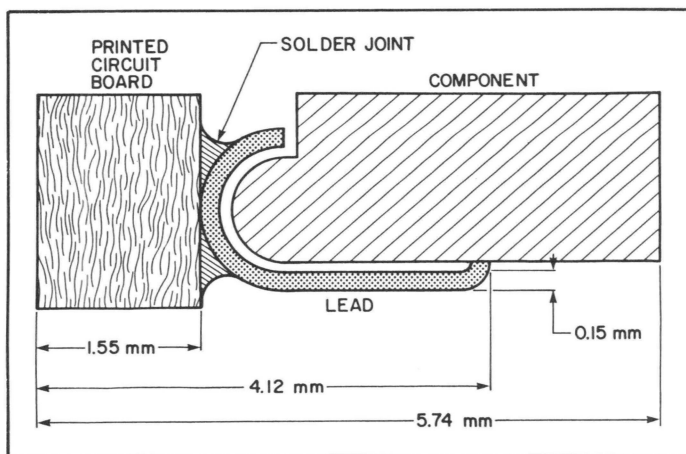


Fig. 3. Cross-sectional geometry and characteristic dimensions of the printed circuit board, the lead, the component, and the solder.

measurements made within the image formed during reconstruction of the heterodyne holograms do relate directly to the component's response to the applied load.

The phase difference measurements made from the heterodyne holograms were, in turn, used to compute displacements and strains along each of the leads of the tested component (Fig. 2), with representative results as detailed in Sec. 5.

5. EXPERIMENTAL RESULTS

The experiments performed in this study were divided into two parts. Part I dealt with the calibration data, with particular emphasis on

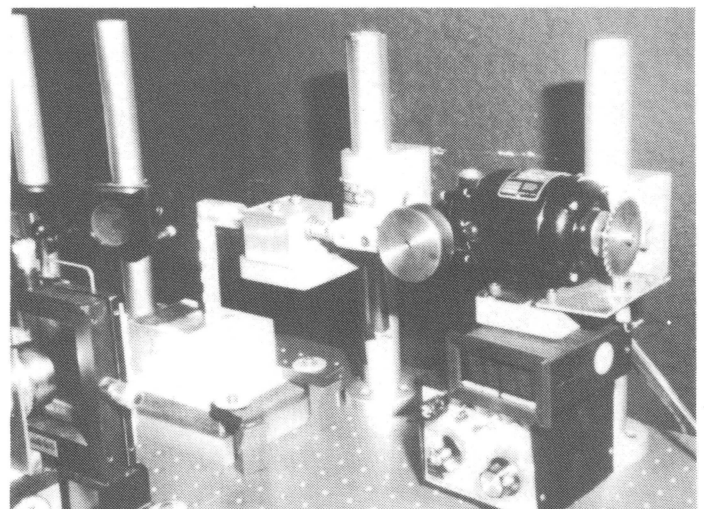


Fig. 4. The loading device: push rod, cam, motor, speed control.

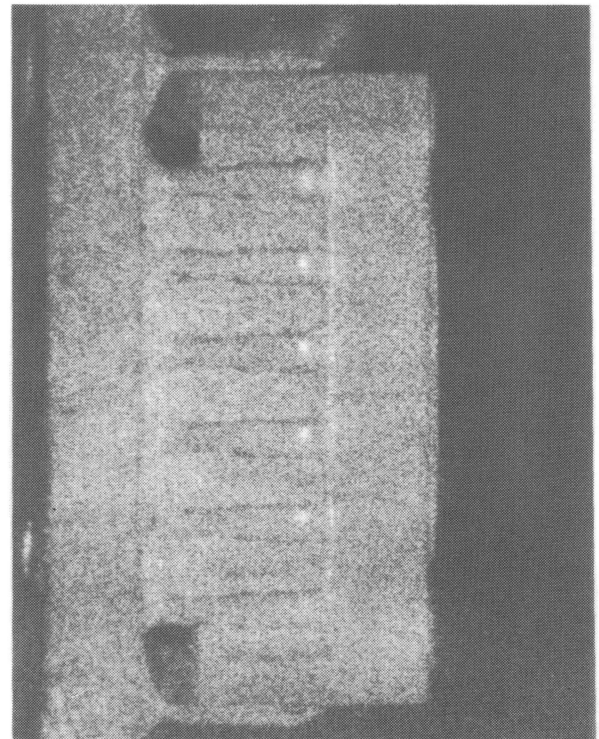


Fig. 5. Image produced during reconstruction of the double-exposure heterodyne hologram of the component board assembly under the condition of no load.

demonstration of the accuracy of the double-exposure heterodyne hologram interferometry as applied to the studies of the component board interaction. Part II dealt with the studies of the load-deformation characteristics of the component leads. Results of Part I and Part II of this study are presented in Secs. 5.1 and 5.2, respectively.

5.1. Calibration data

To demonstrate the accuracy of heterodyne hologram interferometry as applied to the studies of the component board interaction, a double-exposure hologram was recorded, as discussed in Sec. 2, without any load applied to the board. The image reconstructed from this "no-load" double-exposure hologram is shown in Fig. 5. Clearly,

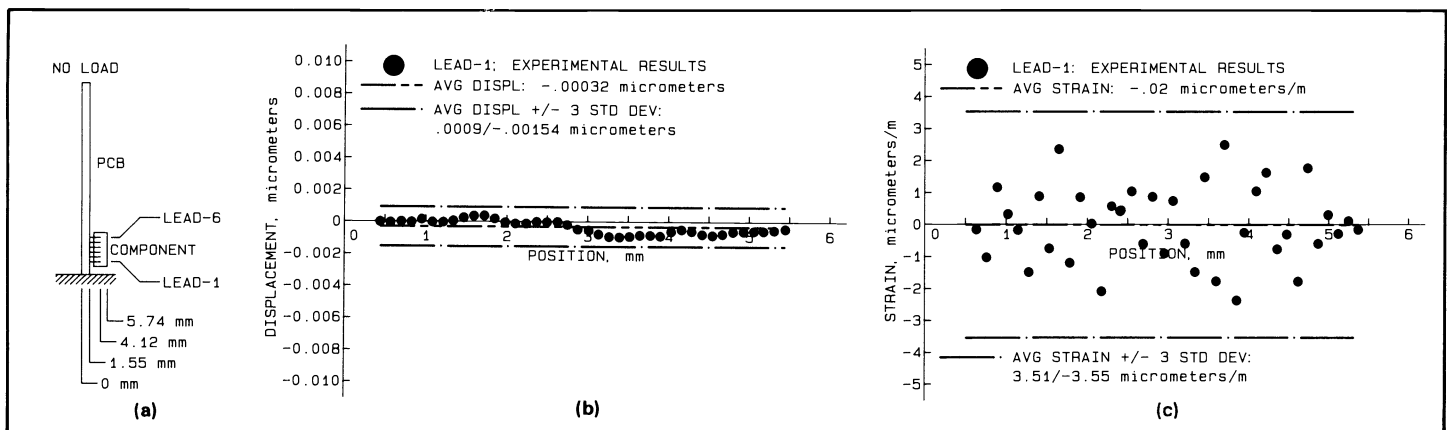


Fig. 6. Calibration data: (a) component board geometry and loading condition, (b) displacement versus position for Lead-1, (c) strain versus position for Lead-1.

no fringes are seen anywhere on the object, indicating no "visible" motion. Therefore, ideally, when the measurements are made from such a hologram, the resulting displacements and strains should be zero. However, due to the optical and electronic noise, some finite phase difference measurements were recorded, which, in turn, have resulted in very small displacements and strains, as shown in Fig. 6.

Figure 6(a) shows the component board geometry and the loading condition, indicating that no load was applied to the board in this case. Figure 6(b) shows displacement versus position for Lead-1 under the no-load condition. Although, for this case, the displacement should ideally be zero, its actual values range between $\pm 0.001 \mu\text{m}$, with the average displacement being $-0.00032 \mu\text{m}$. Statistical analysis of the 40-point displacement data sample [shown in Fig. 6(b)] resulted in the standard deviation of $0.000407 \mu\text{m}$, which for the 99.7% confidence interval (that is, for the interval of \pm three standard deviations) yielded an uncertainty in the displacement measurement of $\pm 0.00122 \mu\text{m}$. In a similar manner, uncertainties in displacement measurements for Lead-2 through Lead-6 were also determined. Examination of these data showed that while using heterodyne hologram interferometry to measure displacements of the component leads, the uncertainty is $0.002 \mu\text{m}$ for the 99.7% confidence interval in the displacement measurement.

Figure 6(c) displays the strain versus position for Lead-1 under the no-load condition. Ideally, for this case, the strain readings should be zero. However, the strains measured from the heterodyne hologram indicate values ranging within $\pm 0.0003\%$ (that is, $\pm 3 \mu\text{m}/\text{m}$), with the average strain of -0.00002% . The statistical analysis of the actual strain, shown in Fig. 6(c), yielded the standard deviation of 0.0001177% , which for the 99.7% confidence interval resulted in an uncertainty of $\pm 0.000353\%$ in the strain measurement. The behavior of the strain versus position data characteristics for Lead-2 through Lead-6 was measured to be similar to that for Lead-1. Based on these results, the overall uncertainty in strain measurement was determined to be 0.0004% .

All in all, for the results presented in this paper, the uncertainty in the displacement measurements is $\pm 0.002 \mu\text{m}$, while the uncertainty in the strain measurement is $\pm 0.0004\%$, based on the 99.7% confidence interval.

5.2. Load-deformation data

To determine the load-deformation characteristics of the leads, a series of double-exposure holograms was recorded under different load conditions and as a function of the number of "load cycles." Typical images obtained during reconstruction of the corresponding holograms are shown in Fig. 7.

It should be noted that similar—in appearance—fringe patterns were obtained for both positive and negative loads applied at the tip of the printed circuit board; the only difference was the sign of the corresponding displacement vector that was reflected in the sign of

the measured phase differences. The holograms were recorded while board flexing was stopped (after the desired number of flexure cycles) at a desired position on the sinusoidal loading cycle. Ideally, these holograms should have been recorded under dynamic loading conditions. However, to do this a pulsed laser would be needed, and one was not available for this study. Therefore, recordings of all holograms were made using a continuous-wave (cw) Ar-ion laser while the board was stationary during the exposures.

To obtain data on load deformation of the component board assembly, holograms were recorded for various magnitudes of deflection at the board's tip, at times corresponding to the specified numbers of accumulated flexure cycles. Representative results corresponding to these holograms are shown in Figs. 8 to 11.

For each of the representative cases, figures giving the summary of the displacement versus position results and strain versus position results, for each of the six leads, are included. The summary figures are useful in determining the displacement/strain trends under given conditions of the test. Furthermore, each of the figures contains a schematic diagram of the board assembly showing the tested component and the specific loading condition for the given representative case [Figs. 8(a), 9(a), 10(a), and 11(a)]. Also shown in these figures are pertinent dimensions indicating locations necessary to establish positions of the board-lead solder joint and the lead-component interface. These positions are shown to be located at 1.55 mm (from the unmounted board surface to the board-lead solder joint) and at 4.12 mm (from the unmounted board surface to the lead-component interface).

Examining Figs. 8(b), 9(b), 10(b), and 11(b), it can be noticed that although there is a minimal displacement at the board-lead solder joint (at 1.55 mm), there is considerable nonzero displacement at the lead-component interface (at 4.12 mm). In general, the outermost leads (that is, Lead-1 and Lead-6) show lower overall displacement than the inner four leads. The maximum displacement at any point on the leads does not exceed $1.2 \mu\text{m}$ for the loads corresponding to the board's tip deflections of $\pm 0.864 \text{ mm}$ ($\pm 0.034 \text{ in.}$). It should be noted that reversing the direction of the load at the board's tip also causes a reversal in the leads' displacement direction. For the cases shown in Figs. 8(b), 9(b), and 10(b), the load was positive and resulted in the leads pushing against the component, which has caused the leads to "buckle" outward, that is, away from the component, in the positive z-direction [Fig. 2(a)]. However, application of the negative load, that is, acting to the left of the board, Fig. 11(b), resulted in the leads pulling the component, which, in turn, has caused the leads to "move" inward, that is, toward the component.

Figures 8(c), 9(c), 10(c), and 11(c) show summaries of the strain distributions along the leads for the four representative test conditions, respectively. The data presented in these figures indicate that there are "rapid" changes in strain levels and directions at the points located at 1.55 mm and 4.12 mm, corresponding to the board-lead

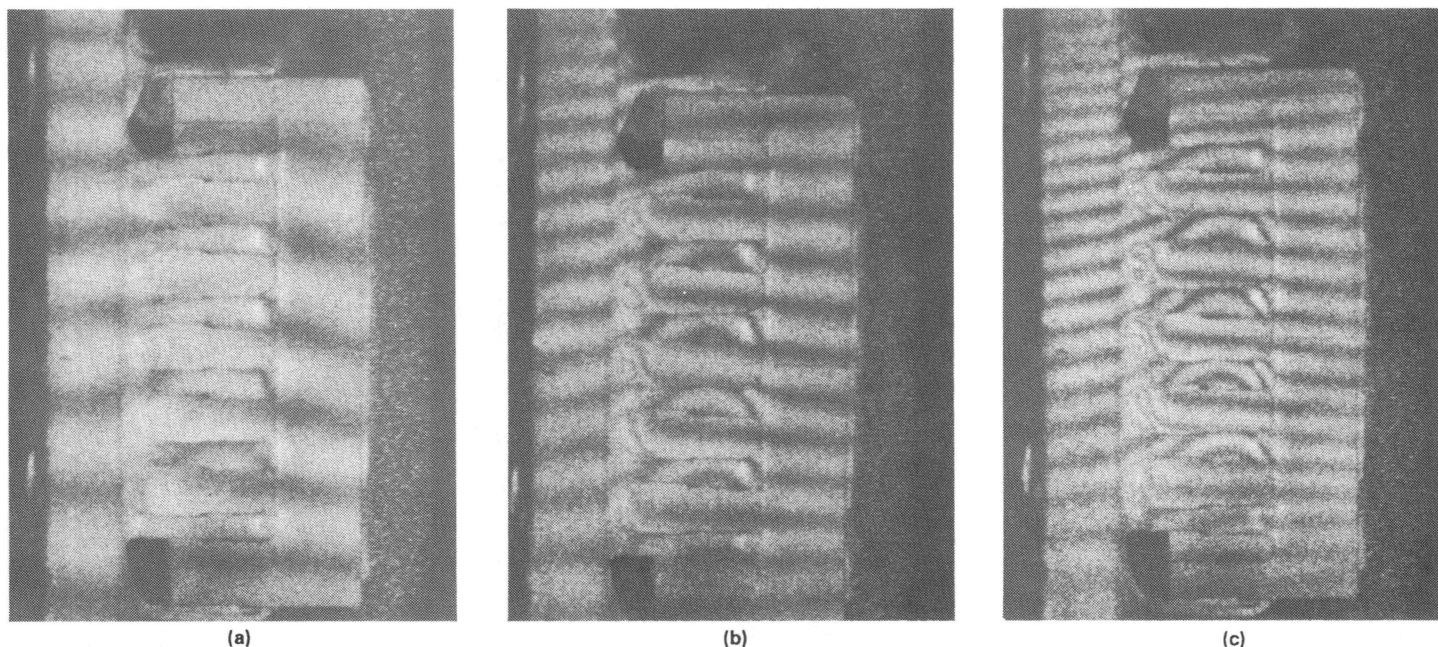


Fig. 7. Images produced during reconstruction of the double-exposure heterodyne holograms of the component board assembly corresponding to deflection at the tip of the board of (a) 0.178 mm (0.007 in.), (b) 0.356 mm (0.014 in.), and (c) 0.864 mm (0.034 in.).

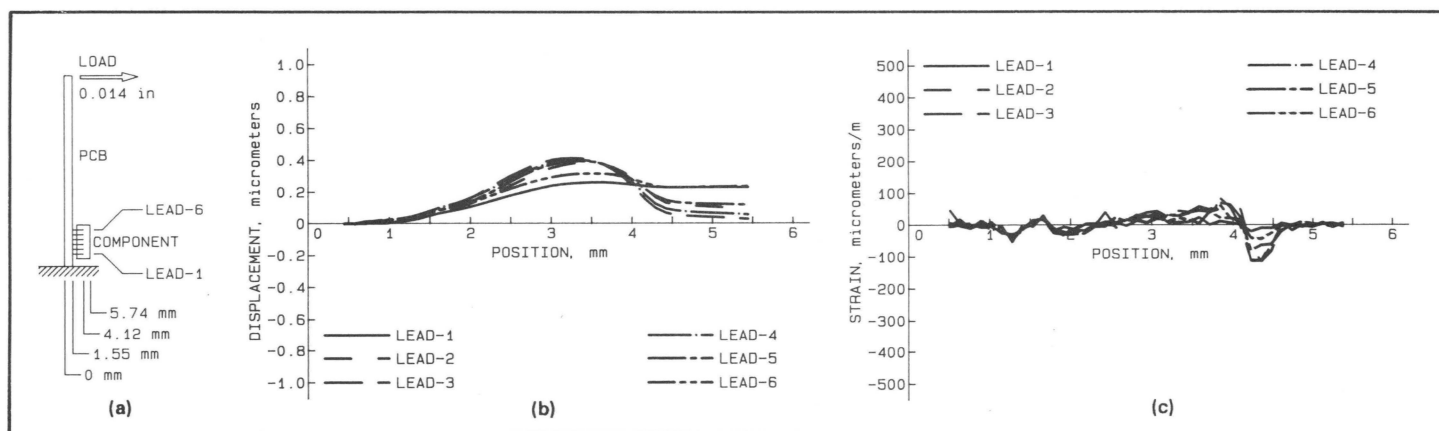


Fig. 8. Summary of experimental results for the load corresponding to the tip of the board deflection of 0.356 mm (0.014 in.) at zero accumulated cycles: (a) component board geometry and loading condition, (b) displacement versus position, (c) strain versus position.

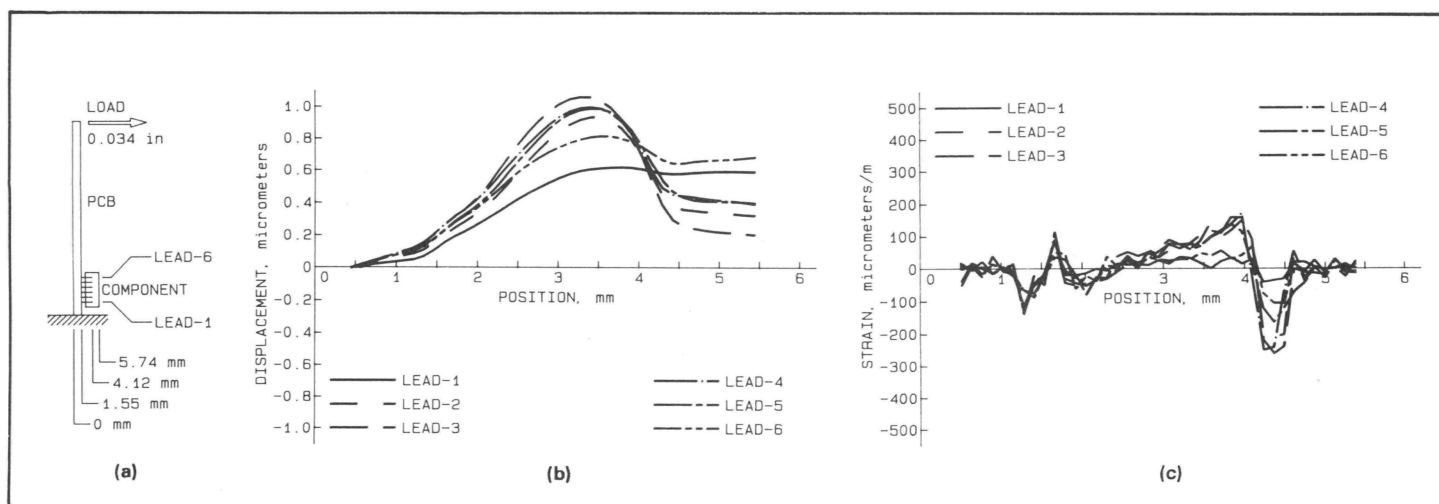


Fig. 9. Summary of experimental results for the load corresponding to the tip of the board deflection of 0.864 mm (0.034 in.) at zero accumulated cycles: (a) component board geometry and loading condition, (b) displacement versus position, (c) strain versus position.

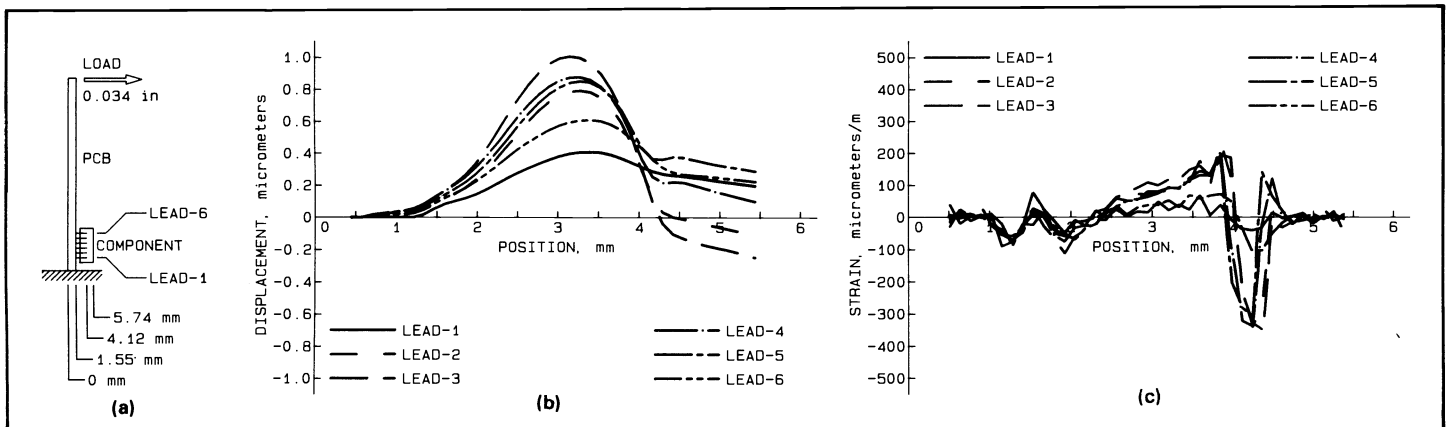


Fig. 10. Summary of experimental results for the load corresponding to the tip of the board deflection of 0.864 mm (0.034 in.) at 100,000 accumulated cycles: (a) component board geometry and loading condition, (b) displacement versus position, (c) strain versus position.

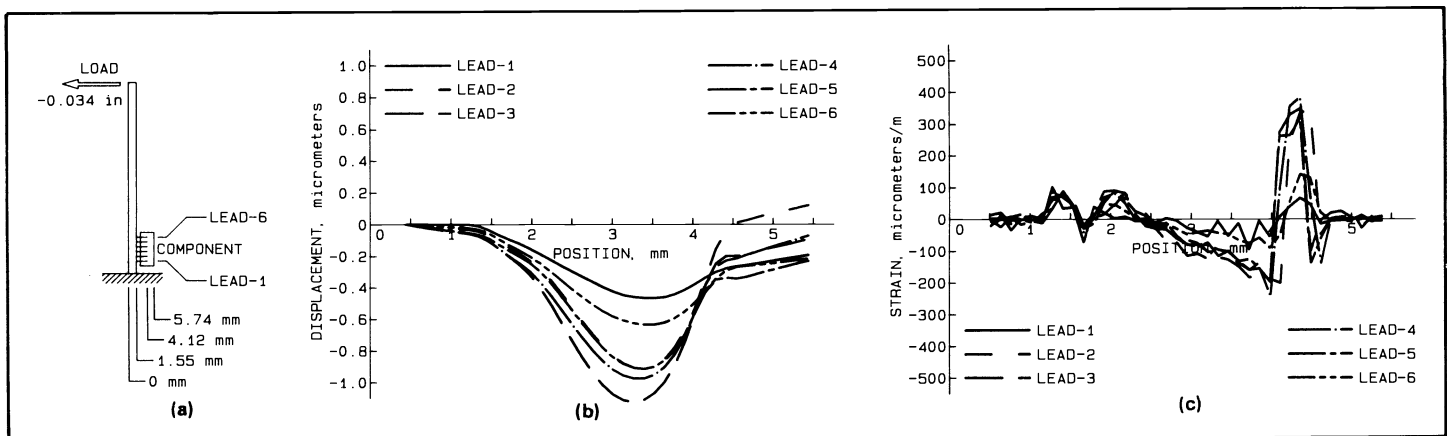


Fig. 11. Summary of experimental results for the load corresponding to the tip of the board deflection of -0.864 mm (-0.034 in.) at 100,000 accumulated cycles: (a) component board geometry and loading condition, (b) displacement versus position, (c) strain versus position.

solder joint and the lead-component interface, respectively. However, the strain distributions along the leads vary approximately linearly. From these data it is seen that strains up to $540 \mu\text{m/m}$ (or 0.054%) were produced at the lead-component interface with substantially lower strains at the board-lead solder joint. The reversal in strain direction is noticeable when comparing the results shown in Fig. 11(c) (negative loading) with the results shown in Figs. 8(c), 9(c), and 10(c) (positive loading).

6. CONCLUSIONS

The results presented in this paper show that displacements and strains due to component board interaction can be measured using the method of double-exposure heterodyne hologram interferometry.

Quantitative interpretation of the double-exposure heterodyne holograms shows that lead displacements on the order of $1.2 \mu\text{m}$ were obtained. Also, the data show that the component moves relative to the board, as evidenced by the nonzero displacements at the lead-component interface.

The experimental results also show that for positive loading the leads deflect *away* from the component, while for negative loading the reverse is true, that is, the leads deflect *toward* the component.

The measured strains were up to $540 \mu\text{m/m}$ for the case of loading

corresponding to the board's tip displacement of $\pm 0.864 \text{ mm}$ ($\pm 0.034 \text{ in.}$). The experimental data indicate that relative magnitudes of strains at the board-lead solder joint are lower than those at the lead-component interface.

The results presented in this paper were obtained for the case of a stationary board; that is, the holograms were recorded while the board flexing device was stopped at a predetermined position to produce the desired deflection at the tip of the board. Ideally, these results should have been obtained using a pulsed laser that would act as an ultrafast "camera" to freeze the board's motion while recording the hologram. In this way, holograms of the component board assembly undergoing the cyclic loading would be recorded under the actual dynamic loading conditions.

All in all, the results presented in this paper show that displacements and strains can be measured along the leads including the board-lead solder joint as well as the lead-component interface. Furthermore, using the method of heterodyne hologram interferometry, these measurements can be made remotely in a noninvasive manner with high accuracy and precision, on the *actual* computer microcomponents. These results for mechanical characteristics of components, together with the results of currently conducted studies of thermal characteristics of the computer components, will constitute an input to the finite element models of computer microcomponents.

⊗